Thermal Control of the New-borns Using a Cascade Approach

Mohamed Aymen ZERMANI*, Elyes FEKI, Abdelkader MAMI

Tunis El Manar University, Faculty of Sciences, El Manar University Campus, 2092, Tunis, Tunisia
mohamedaymen.zermani@fst.utm.tn (**Corresponding author*),
elyes.feki@fst.utm.tn, abdelkader.mami@fst.utm.tn

Abstract: This paper proposes a novel control method for the skin temperature of a preterm new-born and the air temperature and relative humidity of a preterm infant incubator. In the proposed control structure two generalized predictive controllers (GPC) are connected in series with a third GPC for the incubator humidity control. In this paper, a decoupling method is presented, which is meant to reduce the coupling between the infant`s skin temperature and the incubator air space humidity. In order to implement the new proposed controller, a prediction model for an infant incubator with an ultrasonic humidification system was developed. For this purpose, this system was divided into three compartments, namely the preterm infant, the incubator air space, and the active humidification system. Each compartment was modeled by a transfer function using chaotic particle swarm optimization. The effectiveness of the new control structure was compared with that of two other feedback loop-based controllers, namely a simple skin servo-control method (S-GPC) and a skin servo-control cascade method without decoupling (C-GPC). The obtained results demonstrate that the suggested controller performs better than S-GPC and C-GPC in terms of integral absolute error, settling time, response time and disturbance rejection.

Keywords: Neonatal incubator, Mathematical modeling, Skin servo-control, Cascade predictive control.

1. Introduction

Thermal stability in new-borns, especially those who were born very low in weight (VLBW), results from the body's heat production and loss. Previous studies (such as Knobel, 2014; Sherman et al., 2006) have shown that the state of weight gain and caloric intake is not related to the incubation period, but to the thermal stability of the preterm infant and its environment. Therefore, a high-performance controller will be indispensable for neonatal incubators to provide the premature baby with a stable thermal environment similar to that of the womb.

The mechanism of temperature control is one of the most relevant parameters of the incubator. Currently, two control mechanisms are widely used. The first one is skin control mode based on preterm infant skin temperature as a reference, while the second is air control mode based on the air temperature as a reference to control the heating of the incubators. However, each technique has its benefits and drawbacks. For instance, Reddy et al. (2009) in their work, show that the skin control mode results in a significant variation in air temperature, whereas Delanaud et al. (2017) shows that choosing the neutral temperature set point to reduce heat loss was the problem with the air control mode. This complexity is brought about by changes in the incubator's humidity level, the morphology of the premature baby, and the clothing worn in the incubators. Therefore, the control system for the heating power and humidity must be an interactive system in which the new-born participates in the thermal control of its environment.

Numerous studies within the realm of related research are dedicated to enhancing the design of incubators with the aim of improving their affordability and accessibility in developing nations. These endeavours encompass a wide spectrum of incubator optimization facets, including the reduction of manufacturing costs (Donato, 2010), the mitigation of infection risks and power consumption (Tran et al., 2014), and the incorporation of advanced control systems. For instance, Marwanto et al. (2019) delve into the utilization of fuzzy logic as a controller in incubators equipped with temperature and humidity sensors. Their approach seeks to establish a stable and conducive environment for premature infants with low body weight, ultimately bolstering their development and survival prospects.

Meanwhile, Tiwari et al. (2022) investigate the implementation of a real-time control system capable of monitoring and reporting various parameters. This innovation facilitates remote tracking and notifications for caregivers, enhancing the overall care provided to infants. In the work of Alduwaish et al. (2021) the central objective is the deployment of a closed-loop control system in sealed incubators for premature neonates. This system effectively maintains the desired relative humidity (RH) levels, thereby mitigating issues like transcutaneous water loss, dehydration, and

https://doi.org/10.24846/v32i3y202311

excessive cooling, all of which pose significant risks to premature infants. Additionally, Ismail et al. (2021) conduct an investigation into and comparison of the performance of two distinct control systems: a model-free controller (MFC) and a classical proportional-integral-derivative (PID) controller. This study aims to determine the efficacy of these control systems in precisely maintaining the desired temperature inside an incubator. Lastly, Kapen et al. (2019) present their design and implementation of an affordable neonatal incubator equipped with a baby weight monitor, specifically addressing the challenges associated with maintaining incubators in developing countries.

In the literature, most authors have limited their researches to controlling different parameters such as skin temperature, air temperature, or humidity but without interaction between them. For example, Reddy et al. (2009) proposed a fuzzy logic control system that takes into consideration both the infant's body temperature as well as the incubator's air temperature to control the heating, but without humidity control. Zermani et al. (2014) has developed a new active humidification system with a decoupled controller to achieve optimal environmental conditions such as temperature and humidity inside the incubator and to minimize evaporation losses of premature newborns. However, the skin control mode is not considered. Similarly, in the works of Kholiq & Lamidi (2022), Alimuddin et al. (2021), and Sumardi et al. (2019) a control system for infant incubators based on the different structure of a proportional-integral- derivative (PID) controller was proposed for the air control mode, while the skin control mode is not considered. In fact, it's thought that the neonatal incubator system is among those with a relatively slow dynamics and with delay. Therefore, predictive control can be the best sort of control for such systems. Predictive control is an advanced control technique for automation. It can be used to control complex systems, in particular those with long delay times (Morato et al., 2020). The basic idea behind this method is to use a dynamic model of the system running inside the controller to predict its future behavior. Several structures can be used with generalized predictive control. Indeed, in the newborn critical care unit, incubators are frequently subjected to high levels of disruption. The disturbances are largely attributed to the successive interventions by the medical team on preterm babies. Therefore, the use of predictive control with a cascade structure will be an appropriate solution for the regulation of the baby incubator system.

Various mathematical models for new-borns and the incubator process have been established in the literature. Simon et al. (1994) designed a theoretical mathematical model in order to examine the impact of different parameters affecting new-born thermoregulation. Furthermore, recent research on the modelling of incubators has been carried out by Yeler & Koseoglu (2021), where they presented a detailed mathematical model of a modular thermoelectric heat pump system used in a thermoelectric infant incubator. Fraguela et al. (2015) has suggested a mathematical model of the infant in a closed incubator within the first few hours of life. The model of the premature infant was divided into three layers, namely deep tissue, surface tissue, and blood. In their work, the authors have assumed that air temperature and radiant temperature are the control parameters. However, humidity has not been considered. There are also other interesting works on the modelling of new-born incubators that have been developed in the literature such as that proposed by Delanaud et al. (2019).

This work's objective is to present a new control structure for an incubator system. This structure is composed of three GPCs based on three prediction models which are incubator air space, the humidification system, and premature new-born models. Two GPC-based controllers are in cascaded form to simultaneously control the baby's skin temperature and air temperature, and the third one is a conventional GPC for humidity control. Additionally, a decoupling method has been developed to minimize the impact of humidity variation on the premature infant`s temperature. To simulate and predict the outputs of the incubator system, a thermo-dynamic model that requires three compartments is presented. The first one is the infant modelled with two layers - the core and the skin layers. The second compartment is the incubator based on the real measures for the Dräger incubator. The final compartment is the humidification system, that is based on the real measures for the active humidification system. Each compartment is modelled by a transfer function using chaotic particle swarm optimization CPSO. The results from the simulation and actual data for the proposed control algorithm are compared with those of the single-mode GPC controller (S-GPC) and cascade GPC controller (C-GPC) without decoupling.

The rest of this article is organized as follows. In Section 2, the prermature infant incubator system is presented and its numerical model for prediction outputs using (CPSO) is developed. Section 3 proposes a new control method based on cascade generalized predictive control with a decoupling method to improve both the set point tracking and disturbance rejection performances. The simulation and experimental results are presented in Section 4, where the efficacy of the suggested control strategy is illustrated. Section 5 includes the conclusion of this paper and suggestions for additional research.

2. System Description for the Premature Infant Incubator System

Because they are born before some organs have finished developing, preterm new-borns are unable to keep a stable skin temperature outside of a small range of thermal environments. Therefore, these infants must be kept for a specific amount of time in a neutral thermal environment, where they would use the least amount of oxygen and spend the least amount of metabolic energy, as determined by their birth weight and gestational age. Furthermore, when premature babies develop hyperthermia or hypothermia for any reason, their body temperatures need to be closely monitored. In addition to this precise monitoring, it is crucial to provide the infant incubator with necessities like the appropriate temperature and relative humidity that would resemble the environment of the mother's womb. Unlike the different humidification systems of commercial infant incubators, which are often evaporative humidifiers, this study will be carried out on a new nebulization system. The three main components of the active humidification system are the humidification chamber, the fan that is turned on to evacuate humidified air from the incubator through an air passage, and the vapor generator based on an ultrasonic nebulizer.

Figure 1 shows the active humidification system designed to increase and control the humidity level inside the incubator. The operating principle of this system is as follows. A nebulizer provides the suspension of fine droplets of sterile distilled water with a diameter between 2 and 5 pm by ultrasound emission having a frequency around of 2.4 MHz at the level of a piezoelectric ceramic placed on the surface of a water pan. It is important to note that this humidification method has the benefit of producing water vapor at ambient temperatures. Energy consumption is another advantage that makes the use of the ultrasonic humidification process superior to that based on heated components.

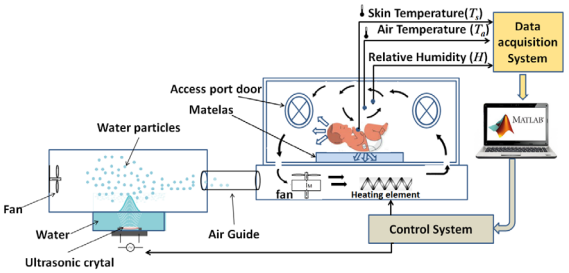

Figure 1. The active humidification system of a closed incubator

2.1 A Thermal Model of an Incubator

There are various models of the premature infant in the literature; however, the models of Simon et al. (1994) and Rojas et al. (1996) are widely used. In this study, we use for simulation the mathematical model developed by Simon with some changes made in the model. The model equations were based on the rule of energy conservation as follows:

$$\frac{dT_c}{dt} = \frac{\mathbb{Q}_{met} - \mathbb{Q}_{sen} - \mathbb{Q}_{lat} - \mathbb{Q}_{cd} - \mathbb{Q}_{bc}}{M_c C_{pc}} \tag{1}$$

$$\frac{dT_s}{dt} = \frac{\mathbb{Q}_{cd} - \mathbb{Q}_{bc} - \mathbb{Q}_{mc} - \mathbb{Q}_{scv} - \mathbb{Q}_{se} - \mathbb{Q}_{sr}}{M_s C_{ps}} \tag{2}$$

$$\frac{dT_w}{dt} = \frac{\mathbb{Q}_{acv} - \mathbb{Q}_{sr} - \mathbb{Q}_{cvo} - \mathbb{Q}_{ro}}{M_w C_{pw}} \tag{3}$$

$$\frac{dT_m}{dt} = \frac{\mathbb{Q}_{mc} + \mathbb{Q}_{mat} - \mathbb{Q}_{ic}}{M_m C_{pm}} \tag{4}$$

Although the model of Simon et al. (1994) can accurately depict this system, it is inappropriate for GPC because of its highly complexity. Therefore, a transfer function model for the preterm new-born, incubator and humidification system are developed using experimental input and output data.

$$TF_1(z) = \frac{\hat{T}_a}{U_1(z)} = z^{-di}\,\frac{b_{0i} + b_{1i}z^{-1} + \cdots + b_{mi}z^{-mi}}{1 - a_{1i}z^{-1} - \cdots - a_{ni}z^{-1}} \tag{5}$$

$$TF_2(z) = \frac{\hat{T}_s}{U_2(z)} = z^{-d_i'}\,\frac{b'_{0i} + b'_{1i}z^{-1} + \cdots + b'_{mi}z^{-mi}}{1 - a'_{1i}z^{-1} - \cdots - a'_{ni}z^{-1}} \tag{6}$$

$$TF_3(z) = \frac{\hat{H}}{U_3(z)} = z^{-d_i''}\,\frac{b''_{0i} + b''_{1i}z^{-1} + \cdots + b''_{mi}z^{-mi}}{1 - a''_{1i}z^{-1} - \cdots - a''_{ni}z^{-1}} \tag{7}$$

where $\hat{T}_S$, $\hat{T}_a$ and $\hat{H}$ are the output values predicted for the skin temperature, air temperature and relative humidity, respectively. U_1, U_2 and U_3 are the control inputs of the transfer functions TF_1, TF_2 and TF_3, respectively and b_{mi}, b'_{mi}, b''_{mi}, a_{ni}, a'_{ni} and a''_{ni} are the unknown system parameters. Identifying the parameters of the above three transfer functions may not be effective if the necessary conditions are not verified in real-world applications. First, the sampling time must be carefully chosen to obtain the correct resolution without it being extreme. In the situation under investigation, a sampling interval of 20 seconds was used to record all experimental data. Second, the system must function under standard settings, which call for a 28°C outdoor temperature and a temperature within the incubator between 30 and 38°C. In addition, the input signal should excite as many modes of the system as possible. This gives the identification process enough details to characterize the system dynamic and static gain. Identification of parameters is made by the minimization of the model output error, as described above. Then, the three proposed cost functions to be minimized are as follows:

$$SSE1 = \sum_{k=1}^{N_{samples}} \hat{T}_a(k) - T_a(k))^2 \quad (8)$$

$$SSE2 = \sum_{k=1}^{N_{samples}} (\hat{T}_S(k) - T_S(k))^2 \quad (9)$$

$$SSE3 = \sum_{k=1}^{N_{samples}} (\hat{H}(k) - H(k))^2 \quad (10)$$

where $N_{samples}$ is the number of samples. Identifying the system's optimal parameters can be done using a variety of approaches. Such heuristic methods as least squares and output error with an extended prediction model generally provide adequate results. However, the meta-heuristic algorithm for the parametric estimation represents a more straightforward option in complex system identification. In this work, chaotic particle swarm optimization (CPSO) will be used to optimize the transfer function parameters.

2.2 Chaotic Particle Swarm Optimization (CPSO)

In the literature, there are several different parametric identification methods. Some authors choose to employ intelligent techniques, as in (e.g. Zaylaa et al., 2018), which uses a backpropagation network for parametric identification. The drawback of all such ANNs is that a large amount of data must be collected in order to train the network accurately. Another heuristic technique, such as least squares method usually gives satisfactory results. Metaheuristic algorithms, however, offer a simpler solution in complex situations. This biologically inspired optimization approach is widely used in many fields. Metaheuristic algorithms have been the subject of many developments and applications (e.g. Zermani et al., 2023). Numerous population-based metaheuristic methods are available that can be modified for parametric estimation. This study proposes the implementation of an enhanced particle swarm optimization algorithm using the chaos theory called CPSO to identify the incubator system transfer functions described in equations (5), (6), and (7). The concept involves using a chaotic sequence generator for obtaining the values of random variables. The logistic equation and other equations, such as the tent map, the Gauss map, the Lozi map, and others, can be adopted instead of random ones. The tent map was used in this study as the chaotic map to create the first population.

The latter is expressed mathematically as follows:

$$x_{k+1} = \begin{cases} \dfrac{x_k}{0.7} & x_k < 0.7 \\ \dfrac{10}{3}(1 - x_k) & otherwise \end{cases} \quad (11)$$

In this case, the range of the chaotic variables is [0 1]. Since the output of the chaotic variable differs from the range of the optimization variable, the chaos search space would be normalized in the range [1, -1] using this equation:

$$Y_i^j = Y_{\min}^j + (Y_{\max}^j - Y_{\min}^j)x_k \quad (12)$$

where $Y_{\max}^j$ and $Y_{\min}^j$ denote the bounds of j^{th} optimization variable. The pseudo-code for CPSO is listed in Algorithm 1, where $rand_1$ and $rand_2$ are uniformly distributed random values in the range [0, 1], w is the inertia weight, and c_1 and c_2 are the acceleration factors. The x_i^t is the current position of the particle, its optimal position is called $pbest_i^t$, the global optimal position is called $pgbest_i^t$, and the partical velocity is v_i^t. The validation of the developed model is defined by three functions: the total correlation coefficient R^2_{Total}, the multiple correlation coefficients R^2_{mult} and the mean square

error (MSE). It can be considered that the model is validated if the MSE is around zero and R^2_{Total} and R^2_{mult} are close to 1.

Algorithm 1 CPSO algorithm

Initialize the parameters (V_{min},V_{max}, X_{max}, X_{min}, c_1, c_2 NP: NumParticles, D: Dimension, MI:max iterations)
Initialize particles x_i by the Tent chaotic map
Repeat
for $i = 1\ toNP$
if $f(x_i) \le f(pbest_i)$
$pbest_i \leftarrow x_i$
if $f(x_i) \le f(pgbest)$
$gpbest_i \leftarrow x_i$
Endif
for $j = 1\ toD$
generate the random values $rand_1$ and $rand_2$ by the Tent chaotic map

$$v_{ij}^{(t+1)} = w^t.v_{ij}^t + c_1 rand_1(x_{ij}^t - pbest_{ij}^t) + c_2 rand_2(x_{ij}^t - pgbest_j)$$

$$v_{ij}^{(t+1)} \in (V_{\min}, V_{\max})$$

$$x_{ij}^{(t+1)} = x_{ij}^t + v_{ij}^{(t+1)}$$

$$x_{ij}^{(t+1)} \in (X_{\min}, X_{\max})$$

End for
End for
Until MI reached
Return $f(pbest)$ *and* $pgbest$

$$MSE(T_i, \hat{T_i}) = \frac{1}{N_{samples}} \sum_{k=0}^{N_{samples}-1} (T_{ik} - \hat{T}_{ik})^2 \quad (13)$$

$$R^2_{mult}(T_i, \hat{T_i}) = 1 - \frac{\sum_{k=0}^{N_{samples}-1} (T_{ik} - \hat{T}_{ik})^2}{\sum_{k=0}^{N_{samples}-1} (T_{ik} - \bar{T}_i)^2} \quad (14)$$

$$R^2_{Total}(T_i, \hat{T_i}) = 1 - \frac{\sum_{k=0}^{N_{samples}-1} (T_{ik} - \hat{T}_{ik})^2}{\sum_{k=0}^{N_{samples}-1} (T_{ik})^2} \quad (15)$$

3. The Control Strategy

Air and skin control are the two control modes used by incubators. Infant clinical characteristics like birth weight, gestational age, and health state are frequently taken into account when choosing an air/skin control mode. Air control, which is more reliable than skin control, cannot lower heat losses, particularly from newborns with very low birth weights. In addition, skin control results in highly fluctuating incubator air temperatures with significant overshoot.

The goal of this section is to build a new way of controlling neonatal incubators in order to prevent heat loss and preserve the thermal equilibrium between the child and its surroundings. As it is illustrated in Figure 2, the general block structure of the new mode of control is based on a cascade generalized predictive controller to control the skin and ambient temperatures added to a conventional GPC to control the humidity. This structure provides the advantages of both skin and air control mode: it allows achieving the desired skin temperature of the premature infant while respecting the range of internal incubator air temperature and with a minimum of coupling with the variation of humidity. In practice, the infant incubator system is usually subject to different constraints, such as the input constraint of the actuator and the operational limits of the system. The actuator saturations of the incubator are the limits of the heater and the humidifier power. For operational and safety considerations, it is often required to keep the temperature inside the incubator under certain limits. Consequently, the choice of constraints in the design of the control is an important step. The control inputs of system are: U_1, which represents the required air temperature, U_2, which represents the heat power, and U_3, which represents the humidifier power. The outputs of the incubator system are: T_1, which represents the skin temperature, T_2, which represents air temperature and T_3, which represents the relative humidity. TF_1, TF_2 and TF_3 represent the transfer functions of the preterm infant, air incubator and active humidification system, respectively. The parameters of the transfer functions are obtained using a system identification based on particle swarm optimization (CPSO) algorithm.

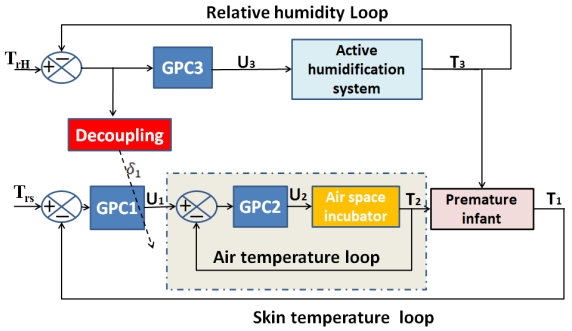

Figure 2. The proposed control structure design for skin servo-control

3.1 The Cascade Predictive Control Law

Predictive control entails taking into account a process's future behavior in the present. This is done by predicting the system's exit in the future on a finished horizon using a numerical model of the system. The purpose of the predictive strategy is to make the output of the process coincide with the set point in the future on a finite horizon. This study proposes a cascade GPC (C-GPC) for air and skin temperature control and a conventional GPC for humidity control. The different loop models are single input, single output (SISO). The air and skin cost functions to be optimized are described by the following equations:

$$J_{GPC1} = \sum_{t=N_{11}}^{N_{21}} \delta_1 \left| \hat{T}_1(k+t) - T_{rs}(k+t) \right| + \sum_{t=1}^{N_{u1}} \lambda_1 \left| \Delta u_1(k+t-1) \right|^2 \quad (16)$$

$$J_{GPC2} = \sum_{t=N_{12}}^{22} \delta_2 \left| \hat{T}_2(k+t) - u_{1op}(k+t) \right| + \sum_{t=1}^{N_2} \lambda_2 \left| \Delta u_2(k+t-1) \right|^2 \quad (17)$$

The humidity cost function to be optimized is described by the following relation:

$$J_{GPC3} = \sum_{t=N_{13}}^{N_{23}} \delta_3 \left| \hat{T}_3(k+t) - T_{rH}(k+t) \right| + \sum_{t=1}^{N_{u3}} \lambda_3 \left| \Delta u_3(k+t-1) \right|^2 \quad (18)$$

where $\hat{T}_1(k+t)$ is the skin temperature predicted at the time $(k+t)$. $T_{rs}(k+t)$ is the skin set point applied at the time $(k+t)$. $\Delta u_1(k+t-1)$ represents the future control increments of external loop at the time $(k+t-1)$.

$\hat{T}_2(k+t)$ is the air temperature predicted at the time $(k+t)$. $u_{1op}(k+t)$ is the air set point applied at the time $(k+t)$. $\Delta u_2(k+t-1)$ represents the future control increments of internal loop at the time $(k+t-1)$.

$\hat{T}_3(k+t)$ is the humidity predicted at the time $(k+t)$. $T_{rH}(k+t)$ is the humidity set point applied at the time $(k+t)$. $\Delta u_3(k+t-1)$ represents the future control increments of humidity loop at the time $(k+t-1)$.

N_{1i} and N_{2i} are the starts and the ends of the prediction horizon, respectively. N_{ui} is the control horizon where i = {1,2,3}. The parameters δ_i and λ_i affect the future behavior of the controlled process. Generally, they are chosen in the form of constants or exponential weights. The result of the minimization of the external criterion provides the optimized sequence of the internal set point. This sequence is then directly reused at the level of the internal minimization to elaborate the command applied to the process. The basic principle of predictive control is to use a numerical model to predict the future behavior of the system. Generally, the model used for prediction is given by the following equation:

$$A_i(z^{-1})T_i(k) = z^{-d_i}B_i(z^{-1})u_i(k-1) + \frac{C_i(z^{-1})}{\Delta(z^{-1})}n_{ci}(k) \quad (19)$$

The optimum prediction structure at time $(k+t)$ will be:

$$T_i(k+t) = \frac{B_i(z^{-1})}{A_i(z^{-1})}u_i(k+t-d_i-1) + \frac{C_i(z^{-1})}{A_i(z^{-1})\Delta(z^{-1})}n_{ci}(k+t) \quad (20)$$

After highlighting future and past values, the prediction model will be as follows:

$$\hat{T}_i(k+t) = G_{t_i}(z^{-1})\Delta(z^{-1})u_i(k+t-d_i-1) + \frac{H_i(z^{-1})}{C_i(z^{-1})}T_i(k) + \frac{R_{t_i}(z^{-1})}{C_i(z^{-1})}\Delta(z^{-1})u_i(k-1) + L_{t_i}(z^{-1})n_{c_i}(k+t) \quad (21)$$

where the unknown polynomials $G_{t_i}(z^{-1})$, $R_{t_i}(z^{-1})$, and $L_{t_i}(z^{-1})$ are the solutions of the Diophantine equations expressed as follows:

$$C_i(z^{-1}) = A_i(z^{-1})\Delta(z^{-1})L_{t_i}(z^{-1}) + z^{-t}H_i(z^{-1}) \quad (22)$$

$$L_{t_i}(z^{-1})B_i(z^{-1}) = C_i(z^{-1})G_{t_i}(z^{-1}) + z^{-t+d_i}R_{t_i}(z^{-1}) \quad (23)$$

The prediction output can be represented as a matrix formulation as follows:

$$\hat{T}_i = \hat{G}_i \tilde{u}_i + \frac{1}{C_i(z^{-1})}\hat{H}_i T_i(k) + \frac{1}{C_i(z^{-1})}\hat{R}_i \Delta u_i(k-1) \quad (24)$$

with the notations:

$$\hat{H}_i = \begin{bmatrix} H_{N1i}(z^{-1}) \\ \vdots \\ H_{N2i}(z^{-1}) \end{bmatrix}, \hat{R}_i = \begin{bmatrix} R_{N1i}(z^{-1}) \\ \vdots \\ R_{N2i}(z^{-1}) \end{bmatrix}$$

$$\hat{u}_i = \begin{bmatrix} \Delta u_i(k) \\ \vdots \\ \Delta u_i(k+Nu_i-1) \end{bmatrix}, \hat{T}_i = \begin{bmatrix} \hat{T}_i(k+N_{1i}) \\ \vdots \\ \hat{T}_i(k+N_{2i}) \end{bmatrix} \quad (25)$$

$$\hat{G}_i = \begin{bmatrix} g_{N_{1i}} & 0 & 0 & \cdots & 0 \\ g_{N_{1i}+1} & g_{N_{1i}} & 0 & \cdots & 0 \\ g_{N_{1i}+2} & g_{N_{1i}+1} & g_{N_{1i}} & \cdots & 0 \\ \vdots & \vdots & \vdots & \ddots & \vdots \\ g_{N_{2i}} & g_{N_{2i}-1} & g_{N_{2i}-2} & \cdots & g_{N_{2i}-N_{ui}+1} \end{bmatrix}$$

The predictions from $d_i + 1$ to $d_i + N_{2i}$ must be determined in order to compute the control action.

3.2 Minimization of the GPC Criterion with Constrained Formulation and Decoupling

The cost functions given in equations (16), (17) and (18) can be converted into the following three formulas:

$$J_1 = (\hat{T}_1 - T_{rs})^T \delta_1 (\hat{T}_1 - T_{rs}) + \lambda_1 \tilde{u}_1^T \tilde{u}_1 = (\hat{G}_1 \tilde{u}_1 + t_1 - T_{rs})^T (\hat{G}_1 \tilde{u}_1 + t_1 - T_{rs}) + \lambda_1 \tilde{u}_1^T \tilde{u}_1 \quad (26)$$

$$J_2 = (\hat{T}_2 - \tilde{u}_1)^T \delta_2 (\hat{T}_2 - \tilde{u}_1) + \lambda_2 \tilde{u}_2^T \tilde{u}_2 = (\hat{G}_2 \tilde{u}_2 + t_2 - \tilde{u}_1)^T (\hat{G}_2 \tilde{u}_2 + t_2 - \tilde{u}_1) + \lambda_2 \tilde{u}_2^T \tilde{u}_2 \quad (27)$$

$$J_3 = (\hat{T}_3 - T_{rH})^T \delta_3 (\hat{T}_3 - T_{rH}) + \lambda_3 \tilde{u}_3^T \tilde{u}_3 = (\hat{G}_3 \tilde{u}_3 + t_3 - T_{rH})^T (\hat{G}_3 \tilde{u}_3 + t_3 - T_{rH}) + \lambda_3 \tilde{u}_3^T \tilde{u}_3 \quad (28)$$

with

$$\delta_i = \begin{pmatrix} \delta_i(t) & 0 \\ 0 & \delta_i(t) \end{pmatrix}, \lambda_i = \begin{pmatrix} \lambda_i(t) & 0 \\ 0 & \lambda_i(t) \end{pmatrix} \quad (29)$$

To obtain a reliable controller for skin temperature regulation with minimal impact of humidity variation on temperature control, a new expression for the weighting factor given by the following formula is established:

$$\delta_1(k) = \begin{cases} \delta_1 \max & \delta_1(k) > \delta_1 \max \\ \beta_1 \exp(|H_r(k) - H(k)| & \delta_1(k) \le \delta_1 \max \end{cases} \quad (30)$$

where β_1 is constant to amplify the error factor. The constraints on the amplitude of the control signal $u_i(k)$ and on the increment signal of the $\Delta u_i(k)$ are important for the incubator system. These constraints can be expressed using the following inequalities:

$$\begin{aligned} u_{i_{\min}} &\le u_i \le u_{i_{\max}} \\ \Delta u_{i_{\min}} &\le \Delta u_i \le \Delta u_{i_{\max}} \end{aligned} \quad (31)$$

where $u_{i_{\min}}$ and $u_{i_{\max}}$ are the minimum and maximum value of control signal that can be reached, respectively. $\Delta u_{i_{\min}}$ and $\Delta u_{i_{\max}}$ represent the minimum and maximum derivative threshold of the control inputs, respectively.

In a multivariable system, process variables are often interconnected, which means that changing one variable can affect others. Decoupling aims to mitigate or eliminate these interactions, allowing each variable to be controlled independently, thus simplifying overall system control.

In the context of predictive control, it can be noticed that using a variable weighting factor on the control increment has a significant impact on control dynamics.

If the weight is high, it means that adjusting this variable is encouraged because it contributes to achieving control objectives.

If the weight is low, it means that adjusting this variable is discouraged because it may have an undesirable impact on other variables or control objectives. Therefore, controlling the weighting factor according to the importance of a variable relative to other variables or control objectives optimizes system performance while minimizing unwanted interactions.

In the proposed system, the impact of humidity variation on evaporation losses is quite significant, and consequently, it affects the baby's skin temperature. To minimize this coupling, the weighting factor δ_1 of GPC1 was adjusted with an exponential function given in equation (30) that depends on the humidity rate variation inside the incubator. By judiciously adjusting the weights of various process variables, the desired thermal balance can be achieved. To sum up, predictive control with decoupling using a variable weighting factor on the control increment is a sophisticated control approach aimed at optimizing the regulation of interdependent variables by adjusting controls to account for effects on the entire system. The variable weights help prioritize adjustments

based on control objectives and the desired or undesired interactions between variables.

The computational complexity of the proposed GPC (Generalized Predictive Control) cascade decoupling algorithm applied to a baby incubator system for controlling air temperature, skin temperature, and humidity can vary depending on several factors:

Incubator System Complexity: The algorithm`s complexity will depend on the specific configuration of the incubator system, including the number of sensors, actuators, and control variables involved in the system;

Prediction Horizons: The chosen prediction horizons for each cascade control loop will impact the algorithm`s complexity. Longer horizons may increase the computational workload;

Modeling Methods: How the system model is constructed can have an impact on the algorithm`s complexity. More detailed and accurate models may require additional calculations;

Optimization and Regulation: The optimization methods used to tune GPC controller parameters may have varying computational requirements. Similarly, simultaneous control of multiple variables can increase the algorithm`s complexity;

Sampling Frequency: The rate at which data is sampled and control actions are updated will influence the computational load. Higher sampling frequencies may require faster computations;

Hardware Resources: Available hardware resources, such as CPU processing power, memory, and communication speed, will play a crucial role in managing the algorithm`s complexity;

Handling Delays: If the system exhibits significant delays, managing them effectively may increase algorithm complexity.

4. Simulation and Experimental Results

The experimental tests carried out in this study are based on the evaluation of a 8000C commercial infant incubator model with a new active humidification system as it is shown in Figure 3. The humidifier system mainly consists of the humidification chamber with a height of 20 cm and a length of 50 cm, a fan that is turned on to evacuate humidified air from the incubator through an air guide and an ultrasonic nebulizer. Temperature and humidity data are collected inside the incubator according to the IEC-60601 standards using two sensors which are LM35 and SY-230.

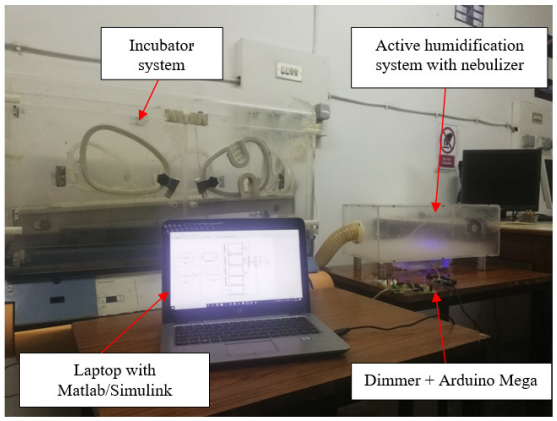

Figure 3. Real process of a neonatal incubator system

4.1 Model Identification

The three developed transfer functions for describing the global incubator system with premature infants were simulated and validated with experimental data. The process of identification provided three subsystems, TF_1, TF_2 and TF_3, represented as follows:

$$\ddot{u}_1 = {}^{-70}\frac{\aleph 6.28881\ddot{u}\quad 0.5^{-1}\quad 0.00012861^{-2}}{1-1.202281z^{-1}+0.20404z^{-2}} \tag{32}$$

$$\ddot{u}_2 = {}^{-17}\frac{-0.0013719z^{-1}+0.02391631z^{-2}}{1-0.8521z^{-1}+0.1381z^{-2}} \tag{33}$$

$$\ddot{u}_3 = {}^{-1}\frac{-0.0087429z^{-1}+0.0084278z^{-2}}{1-0.1694z^{-1}+0.78528z^{-2}} \tag{34}$$

As it is shown in Figures 4, 5 and 6, the three transfer functions TF_1, TF_2 and TF_3 that were identified using CPSO were close to real system behavior. The values of CPSO parameters are the following: the population size is equal to 500, the velocity is constant, c_1 and c_2 are equal to 2 and the number of iterations is equal to 100. Three validation indices which are the total correlation coefficient, the multiple correlation coefficients and the mean square error are used. The obtained values for these indices are included in Table 1, it can be noticed that R^2_{Total} and R^2_{mult} are close to 1, and the MSE was rounded to zero. Consequently, TF_1, TF_2, and TF_3 were acceptable as models for

the skin temperature of the premature infant, the incubator air space temperature, and the humidity rate inside the incubator, respectively.

Table 1. The values of the validation indices

Validation	TF_1	TF_2	TF_3
R^2_{Total}	0.995203	0.999236	0.973919
R^2_{mult}	0.993880	0.988969	0.905281
MSE	0.002039	0.0186290	0.2101673

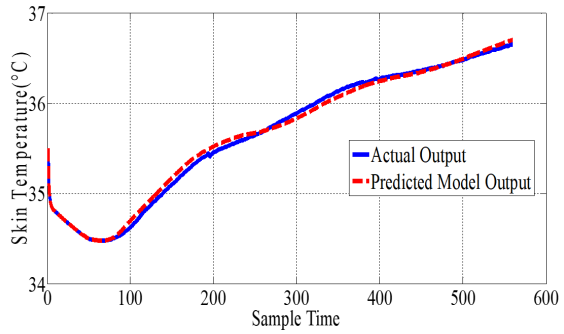

Figure 4. Real and estimated skin temperature of the premature infant (T_1)

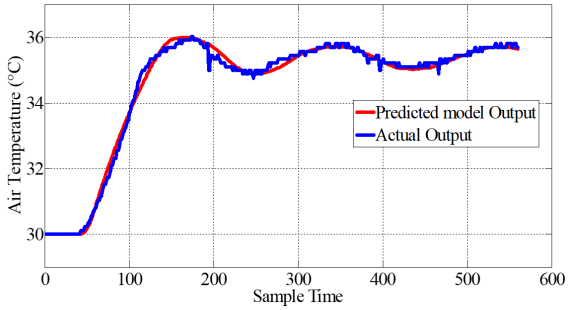

Figure 5. Real and estimated air temperature of the incubator system (T_2)

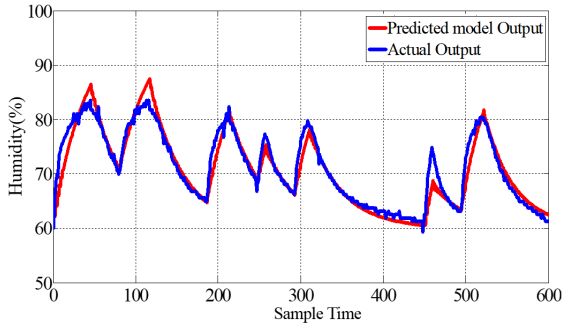

Figure 6. Real and estimated relative humidity (H) inside the incubator

4.2 Evaluating the Performance of the Cascade Control Strategy

The main parameters that have been involved in the design of a GPC controller are $HP_i = (N_{2i} - N_{1i})$, λ_i and the δ_i. These parameters have an important role in defining the closed-loop system dynamics. To ensure that the system under study behaves as expected, various parameters were tested, and only the best ones were selected and used for different control structures. As it is detailed in Table 2, which lists the parameter values for the three control structures employed, these carefully chosen values played a crucial role in achieving the desired system performance.

Table 2. Parameters values for the three control structures employed

	S-GPC	C-GPC	CD-GPC
HP_1	100	100	100
HP_2	-	60	60
HP_3	60	60	60
δ_1	1	1. 382	f(e(k))
δ_2	-	1	1
δ_3	20	20	20
λ_1	0.009	0.435	0.435
λ_2	-	0.1	0.1
λ_3	3.4	3.4	3.4
min< U_1<max	[0, 100]	[31,37.5]	[31,37.5]
min< U_2<max	-	[0,100]	[0,100]
min< U_3<max	[0,100]	[0,100]	[0,100]

All controllers have the same sampling time, which is equal to 20 seconds. In the context of the simulation results, the vital parameters for the premature baby are presented as the infant`s skin temperature, the air temperature, and the humidity inside the incubator. The GPC controller was applied to the incubator system with a single-mode and cascade structure, with and without the decoupling method. For the validation processes, the environmental temperature T_e was assumed to be 31°C.

Likewise, the initial temperature of the incubator air space T_a, the wall temperature T_w, and the mattress temperature T_m were assumed to be 31°C. On the other hand, the initial temperature of the infant's skin was determined to be 35.5°C. Further on, some results for applying the aforementioned control laws to the infant incubator system are presented.

The skin servo-control mode was simulated with the S-GPC, C-GPC, and CD-GPC controllers. Figure 7(a) displays the evolution of the infant`s skin temperature. Using the C-GPC and CD-GPC controllers, the skin temperature reached the desired value of 37°C without fluctuations and with a small overshoot of 0.09°C. However, with

the single-mode controller, the skin temperature reached the desired value of 37°C after certain oscillations with a significant overshoot of 0.16°C. Figure 7(b) shows the evolution of the air temperature in cascade and single controller modes using S-GPC, C-GPC, and CD-GPC. In cascade mode (C-GPC and CD-GPC), the air temperature rose rapidly in 64 minutes to 37.51°C, which is the constraint output, and remained constant until it reached the NT set point. Then, the air temperature properly followed the NT set point, which is the output of the C-GPC controller, to be stable at thermal neutrality. In Figure 7(b), too, the single-mode controller (S-GPC) features a fast dynamics of the air temperature but with a large overshoot. As a result, the air temperature rises quickly to 40.76°C in 87 minutes before dropping to 34°C with a large fluctuation.

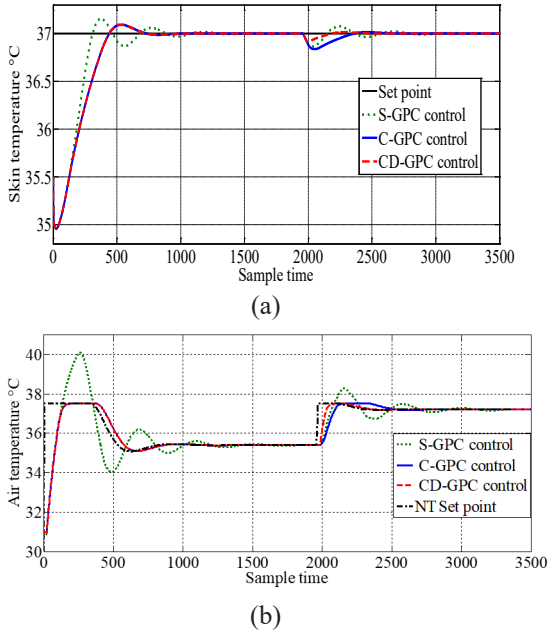

Figure 7. The variation of (a) the preterm infant`s skin temperature and (b) the incubator air temperature using S-GPC, C-GPC, and CD-GPC

To illustrate the coupling effect between humidity and the preterm infant`s skin temperature, a scenario is proposed in which the relative humidity of the air decreases by 20% at a sampling time equal to 2000, as it is shown in Figure 10. It was noticed that to maintain skin temperature at 37°C, an incubator air temperature of 37.25°C was required, which represents an increase of 1.75°C (35.5°C at a humidity rate of 80% to 37.25°C at a humidity rate of 60%). The outcomes of this simulation support those of Delanaud et al. (2019). Figure 8 illustrates the variation of the control signal of the heater using S-GPC, C-GPC, and CD-GPC. Figure 9 illustrates the variation of the GPC1 weighting factor, which is well synchronized with the change of the humidity set point, thus reducing the coupling effect. Figure 10 depicts the humidity response using the conventional GPC control. Figure 11 illustrates the variation of the control signal of the active humidifier.

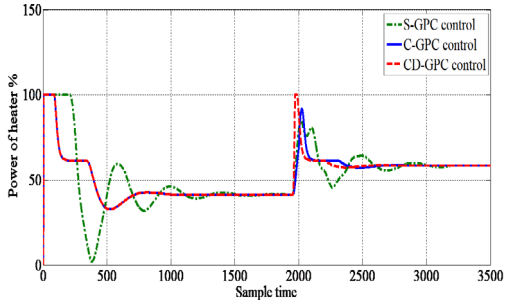

Figure 8. The variation of the control signal of the heater using S-GPC, C-GPC, and CD-GPC

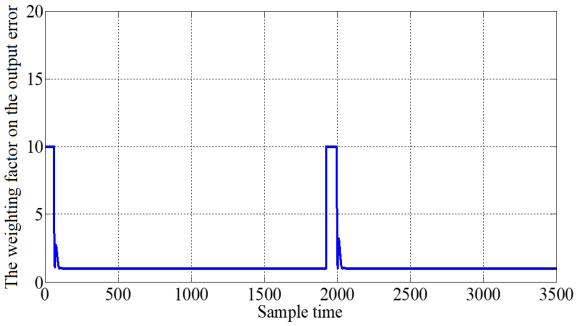

Figure 9. The variation of the GPC1 weighting factor, synchronized with the change of the humidity set point

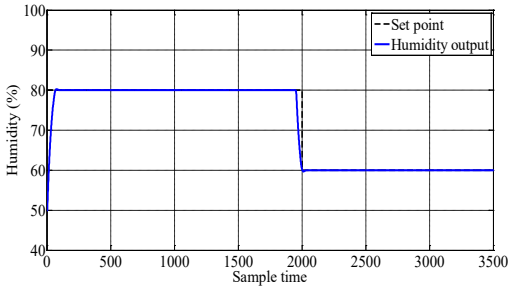

Figure 10. Humidity response using the conventional GPC control

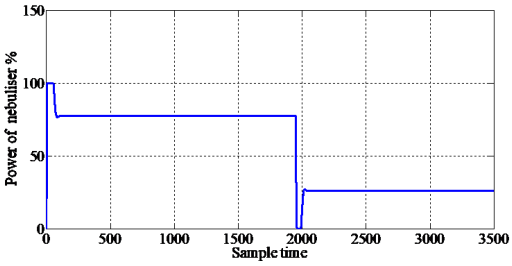

Figure 11. The variation of the control signal of the active humidifier

In Table 3, the performance of the S-GPC, C-GPC, and CD-GPC methods is illustrated using indices that include IAE1 and IAE2 for T_s (the skin temperature) and T_a (the temperature of the incubator air space), respectively, and IAE3 for Skin disturbance rejection. The overshoot for T_s and the temperature of the incubator air space is denoted by T_{ps} and T_{pa}, respectively. The settling time of T_s is denoted by T_{ss} and the time to reach the neutral temperature is denoted by T_{nt}. The proposed controller performs far better than S-GPC and C-GPC. In comparison with S-GPC and C-GPC, the values obtained by the suggested method for IAE1, IAE2, IAE3, T_{ss}, T_{nt}, T_{ps}, and T_{pa} are the smallest for set point tracking and disturbance rejection. These findings show that the suggested approach features a smooth response, no overshoot, and no sustained error.

Table 3. The comparative performance of S-GPC, C-GPC and CD-GPC for different indices

Performance indices	S-GPC	C-GPC	CD-GPC
IAE1	452,22	410,53	410,53
IAE2	1257,81	721,25	706,03
IAE3	35,72	36,96	12,54
T_{ss}	330	233	233
T_{nt}	364	267	267
T_{ps}	0,16°C	0.09°C	0.09°C
T_{pa}	40.76	37.51	37.51
Oscillations	Present	NIL	NIL

While the proposed method may seem promising, it is imperative to acknowledge its reliance on the assumption of linear time invariance within the system dynamics. In real-world applications, this assumption might not always align with the complexities of thermal control scenarios. The presence of nonlinearities and time-varying characteristics can significantly impact control performance, potentially rendering this approach less effective in such instances unless substantial modifications are made to accommodate these challenges.

5. Conclusion

This work presents a novel skin servo-control method for an infant incubator system with an ultrasonic humidifier. The proposed skin servo-control approach (CD-GPC) is based on a decoupling mechanism and a cascade GPC controller. To anticipate the future process behavior, a model of the system was also developed. Simulation results have demonstrated the superiority of the proposed CD-GPC in comparison with the conventional GPC and C-GPC. Moreover, this paper discussed the importance of the new proposed control structure in maintaining the thermal stability of the preterm infant. The control performance evaluation was thoroughly carried out with regard to the performance indices IAE1, IAE2, IAE3, Tss, Tnt, Tps, and Tpa. Clearly, CD-GPC performed better than S-GPC with regard to all performance indices and its performance is almost equal to that of C-GPC. In conclusion, the CD-GPC method can be considered a promising solution for the optimal skin servo-control of a premature newborn. Nevertheless, future research will concentrate on refining the control approach developed in this study. For example, adaptive control could be also introduced in the CD-GPC.

REFERENCES

Alduwaish, S., Alshakri, O., Alamri, R., Alfarieh, R., Alqahtani, S., Hameed, K. & Alomari, A. (2021) Automated humidity control system for neonatal incubator. *Journal of Physics: Conference Series.* 2071, 012029. doi: 10.1088/1742-6596/2071/1/012029.

Alimuddin, A., Arafiyah, R., Saraswati, I., Alfanz, R., Hasudungan, P. & Taufik, T. (2021) Development and Performance Study of Temperature and Humidity Regulator in Baby Incubator Using Fuzzy-PID Hybrid Controller. *Energies*. 14(20), 6505. doi: 10.3390/en14206505.

Delanaud, S., Chahin Yassin, F., Durand, E., Tourneux, P. & Libert, J.-P. (2019) Can Mathematical Models of Body Heat Exchanges Accurately Predict Thermal Stress in Premature Neonates? *Applied Sciences*. 9(8), 1541. doi: 10.3390/app9081541.

Delanaud, S., Decima, P., Pelletier, A., Libert, J. P., Durand, E., Stephan-Blanchard, E., Bach., V. & Tourneux, P. (2017) Thermal management in closed incubators: New software for assessing the impact of humidity on the optimal incubator air temperature. *Medical Engineering & Physics*. 46, 89-95. doi: 10.1016/j.medengphy.2017.06.002.

Donato, K. (2010) Infant Incubator Project: A low-cost, low-energy consumption solution for infant incubators in developing countries. https://jscholarship.library.jhu.edu//handle/1774.2/34130.

Fraguela, A., Matlalcuatzi, F. D. & Ramos, Á. M. (2015) Mathematical modelling of thermoregulation processes for premature infants in closed convectively heated incubators. *Computers in biology and medicine*. 57, 159-172. doi: 10.1016/j.compbiomed.2014.11.021.

Ismail, A., Noura, H., Harmouch, F. & Harb, Z. (2021) Design and control of a neonatal incubator using model-free control. In: *2021 29th Mediterranean Conference on Control and Automation (MED), 22-25 June, 2021, Puglia, Italy*. IEEE. pp. 286-291.

Kapen, P. T., Mohamadou, Y., Momo, F., Jauspin, D. K. & Anero, G. (2019) An energy efficient neonatal incubator: mathematical modeling and prototyping. *Health and Technology*. 9, 57-63. doi: 10.1007/s12553-018-0253-3.

Kholiq, A. & Lamidi, L (2022) Analysis of Temperature Sensors with Proportional and Derivative Controls Applied to Infant Incubators. *Journal of Biomimetics, Biomaterials and Biomedical Engineering*. 55, 216-225. doi: 10.4028/p-f9uc3z.

Knobel, R. B. (2014) Thermal stability of the premature infant in Neonatal Intensive Care. *Newborn and Infant Nursing Reviews*. 14(2), 72-76. doi: 10.1053/j.nainr.2014.03.002.

Marwanto, A., Sunriyadi, K. & Alifah, S. (2019) Fuzzy ogic Implementation For Incubator Prototype With Temperature And Humidity Control. In: *2019 6th International Conference on Electrical Engineering, Computer Science and Informatics (EECSI), 18-20 September, 2019, Bandung, Indonesia*. IEEE. pp. 71-74.

Morato, M. M., Normey-Rico, J. E. & Sename, O. (2020) Model predictive control design for linear parameter varying systems: A survey. *Annual Reviews in Control*. 49, 64-80. doi: 10.1016/j.arcontrol.2020.04.016.

Reddy, N. P., Mathur, G. & Hariharan, S. (2009) Toward a fuzzy logic control of the infant incubator. *Annals of Biomedical Engineering*. 37(10), 2146-2152. doi: 10.1007/s10439-009-9754-6.

Rojas, R. D., Bell, E. F. & Dove, E. L. (1996) A mathematical model of premature baby thermoregulation and infant incubator dynamics. *WIT Transactions on Biomedicine and Health*. 3, 23-38. doi: 10.2495/BSIM960031.

Sherman, T. I., Greenspan, J., Clair, N. S., Touch, S. & Shaffer, T. (2006) Optimizing the neonatal thermal environment. *Neonatal Network*. 25(4), 251-260. doi: 10.1891/0730-0832.25.4.251.

Simon Jr., B. N., Reddy, N. P. & Kantak, A. (1994) A theoretical model of infant incubator dynamics. *Journal of Biomechanical Engineering*. 116(3), 263-269. doi: 10.1115/1.2895729.

Sumardi, Darjat, Sinuraya, E. W. & Pamungkas, R. J. (2019) Design of Temperature Control System for Infant Incubator using Auto Tuning Fuzzy-PI Controller. *International Journal of Engineering and Information Systems (IJEAIS)*. 3(1), 33-41.

Tiwari, R., Raina, G. & Semwal, S. (2022) An Innovative Approach to Neonatal Intensive Unit Care System for New Born babies. In: *2022 International Conference on Advances in Computing, Communication and Materials (ICACCM), 10-11 November, 2022, Dehradun, India.* IEEE. pp. 1-6.

Tran, K., Gibson, A., Wong, D., Tilahun, D., Selock, N., Good, T., Ram, G., Tolosa, L., Tolosa, M., Kostov, Y., Woo, H. C., Frizzell, M., Fulda, V., Gopinath, R., Shashidhara Prasad, J., Sudarshan, H., Venkatesan, A., Sashi Kumar, V., Shylaja, N. & Rao, G. (2014) *Designing a low-cost multifunctional infant incubator.SLAS Technology*. 19(3), 332-337. doi: 10.1177/2211068214530391.

Yeler, O. & Koseoglu, M. F. (2021) Performance prediction modeling of a premature baby incubator having modular thermoelectric heat pump system. *Applied Thermal Engineering*. 182, 116036. doi: 10.1016/j.applthermaleng.2020.116036.

Zaylaa, A. J., Rashid, M., Shaib, M. & El Majzoub, I. (2018) A Handy Preterm Infant Incubator for Providing Intensive Care: Simulation, 3D Printed Prototype, and Evaluation. *Journal of Healthcare Engineering*. 2018, 8937985. doi: 10.1155/2018/8937985.

Zermani, A., Manita, G., Feki, E. & Mami, A. (2023) Hardware implementation of particle swarm optimization with chaotic fractional-order. *Neural Computing and Applications*. 35, 11249-11268. doi: 10.1007/s00521-023-08295-5.

Zermani, M. A., Feki, E. & Mami, A. (2014) Building simulation model of infant-incubator system with decoupling predictive controller. *IRBM*. 35(4), 189-201. doi: 10.1016/j.irbm.2014.07.001.